ACS APPLIED NANO MATERIALS

www.acsanm.org Article

Extreme Thermal Stability and Dissociation Mechanisms of Purified Boron Nitride Nanotubes: Implications for High-Temperature Nanocomposites

Mehul J. Tank, Aspen N. Reyes, Jin Gyu Park, Lyndsey R. Scammell, Michael W. Smith, Ana De Leon, and Rebekah D. Sweat*

Cite This: *ACS Appl. Nano Mater.* 2022, 5, 12444−12453 Read Online

ACCESS | Metrics & More | Article Recommendations | Supporting Information

ABSTRACT: A fundamental understanding of the thermal behavior of reinforcement materials is crucial to fully exploit their properties in composites. Boron nitride nanotubes (BNNTs), structural analogues to carbon nanotubes, are a strong candidate for nanofillers in high-temperature composites due to their high thermal stability, oxidation resistance, excellent mechanical properties, and high thermal conductivity. In this paper, samples of high-quality, high-purity BNNTs were tested to thermal failure in an inert atmosphere for the first time up to 2500 °C. A significant fraction of the BNNTs survived temperatures as high as 2200°, and the BNNT samples were completely undamaged at temperatures as high as 1800 °C. Boron nitride (BN) nanopowders were tested identically to perform a comparative study, as hexagonal BN is commonly found in purified BNNT samples. Observed color darkening, significant weight loss, an increased boron atomic level, significant weight gain upon oxidation, the presence of boron oxide compounds in an oxidized sample, and the observed boron clusters at the nanoscale indicate dissociation of B-N bonds in the BNNT sample at 2200 °C. The stability of BNNT structures was observed up to 2000 °C, with local/partial wall dissociation or unzipping, and complete survivability of highly crystalline BNNTs is demonstrated up to 1800 °C. This paper presents the first-ever study on extreme temperature thermal stability of purified BNNTs in an inert atmosphere analogous to manufacturing processes for high-temperature nanocomposites.

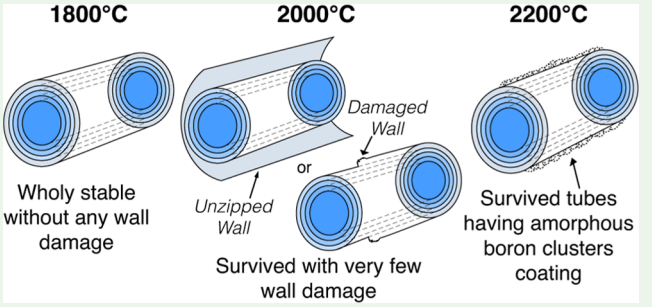

KEYWORDS: *boron nitride nanotubes, decomposition mechanisms, extreme temperature, thermal stability, furnace heating, inert environment*

INTRODUCTION

Following the discovery of carbon nanotubes (CNTs) in the early 1990s, tubular structures of boron nitride were theorized in 1994.[1,2] The BN tubular structure is similar to the hexagonal lattice structure seen in sp^2-hybridized carbon−carbon bonds of graphene and CNTs. The first successful synthesis and observation of BNNTs occurred in 1995, becoming the first inorganic nanotube.[3] Due to their structure, BNNTs possess excellent mechanical properties similar to CNTs. With a tensile strength of 33 GPa,[4] Young's modulus of 1.3 TPa,[5,6] a bending modulus of 760 GPa,[7] and a shear modulus of 7 GPa,[7] they are an obvious candidate for fiber-reinforced composite materials. Along with nanofiller candidate, BNNTs have potential application in hydrogen storage, water purification, and biomedical such as anticancer drug delivery and tissue engineering.[8,9]

In addition to their excellent mechanical properties, BNNTs are more thermally stable in oxidative environments than CNTs.[10,11] Many studies have shown that BNNTs remain stable up to 850 °C in air.[12,13] The thermal stability of BNNTs has also been studied through Joule heating under vacuum by Ghassemi et al.[14] It was estimated that the dissociation of the B−N bond and failure of nanotubes occurred at temperatures up to 1900 °C depending on tube geometry. The boron was evaporated by the Joule heating, causing the dissociation of the bond, and nitrogen was evaporated and carried away by the vacuum.[14] A similar result and mechanism were achieved by Xu et al.[15] via Joule heating of a single nanotube. These studies were conducted through electrical heating and a vacuum atmosphere, having the simultaneous effect of Coulomb force and temperature on the dissociation of BN bonds. However, no reports have explored the temperature stability of BNNTs through a furnace, more similar to a realistic manufacturing

Received: May 5, 2022
Accepted: August 15, 2022
Published: August 25, 2022

https://doi.org/10.1021/acsanm.2c01965
ACS Appl. Nano Mater. 2022, 5, 12444−12453

environment, in an inert atmosphere to study degradation behavior and thermal stability.

Since 1995, much research has been conducted to improve synthesis methods, purification methods, and the implementation of mass production. Although large-scale manufacturing of BNNTs has become feasible, purification is still a concern. The as-grown BNNTs often contain impurities such as metallic catalysts, unreacted precursors, and non-tubular BN compounds.[16] Several methods have been developed and adopted to synthesize BNNTs without metal catalysts producing the as-grown BNNTs containing ∼50% of various boron derivatives. Boron and boron oxides may be removed from BNNTs using well-proven techniques. BN impurities are chemically stable and oxidation-resistant, similar to BNNTs, and so, they are more difficult to remove than boron and boron oxide.

The BNNTs used in this study were provided by BNNT materials, a commercial supplier using the high-temperature-pressure (HTP) method for production.[16] HTP BNNTs are grown by exposing liquid boron droplets to a high-pressure nitrogen environment where BNNTs then evolve via a vapor−liquid−solid pathway. They commonly have 2−5 walls and contain unreacted boron and BN compounds as byproducts/impurities. The as-grown, unpurified BNNTs have a dark brownish-gray appearance, while purified quantities are white.[17] About 50 weight % of the purified BNNTs contain non-tubular boron nitride structures, most commonly hexagonal boron nitride (h-BN). Since BNNTs and h-BN both have an alternating pattern of boron and nitrogen, they have the same compositional makeup of approximately 50% boron atoms and 50% nitrogen atoms. This corresponds to a weight composition of 43.6% boron and 56.4% nitrogen. Although BNNTs and h-BN share the same composition and bonding, they may exhibit different thermal behavior due to different structures; therefore, the h-BN powder is used to perform a comparative study to determine the effect of high temperature on BNNTs. While h-BN has the same elemental makeup and similar thermal conductivity, electrical, and radiation protection properties, it does not contribute to the mechanical properties in composites to the extent nanotubes are capable.

Understanding BNNT behavior at high temperatures will lead to effective manufacturing of composites that employ high-temperature processing matrices, like ceramics. Boron is a low-z element with potential as a neutron radiation shielding material, as deep space exploration and exoplanetary exploration will become a reality in the near future.[18,19] In addition to broadening the matrix and manufacturing possibilities, high-temperature reinforcement materials will be increasingly important in these extreme environments where multifunctional materials are required. Therefore, we present the first-ever study on extreme temperature thermal stability of purified BNNTs in an inert atmosphere analogous to manufacturing processes for metal matrix and ceramic matrix nanocomposites (Scheme 1).

EXPERIMENTAL SECTION

For this study, purified few-walled BNNTs (2−3 walls most common) were provided by BNNT materials. Samples were dried at 200 °C for 2 h prior to heat treatment to remove any excess moisture. Boron nitride nanopowder (h-BN) with an average particle size ≤150 nm was purchased from Sigma-Aldrich and used as received. For more structural details on h-BN used in the study, the scanning electron microscopy (SEM) images taken during the test are provided in the Supporting Information Figure S1. BNNTs and h-BN powder were heated in a high-temperature graphitic furnace (Thermal Technologies HP-4560-20) at a ramp rate of 20 °C/min to the specified temperature and held isothermally for 20 min in a flowing helium atmosphere. Around 50−65 mg of samples was heated in a pre-baked graphite crucible of about 15 mm diameter. The crucible was subjected to a bake-out run at 2500 °C with a hold of 20 min before furnace testing. Weight loss during the furnace heating experiment is calculated from the difference between the measured weight of the sample inside the crucible before and after the test. The crucible used in the furnace testing experiment is ∼1000 times heavy compared to the sample mass (∼60 g of crucible vs ∼60 mg s of BNNT sample), the slight change in the crucible mass during the experiment will show up as a considerable number in the weight measurement of the sample. To overcome this weight measurement limitation of the high-temperature furnace, we further performed high-temperature thermogravimetric analysis (HT-TGA) to get precise weight loss data. HT-TGA for BNNTs was performed in a Netzsch STA 449 F1 Jupiter in a graphite crucible heated from room temperature to 2050 °C.

Scheme 1. Thermal Decomposition Mechanism Studies of Furnace-Heated BNNTs and hBN

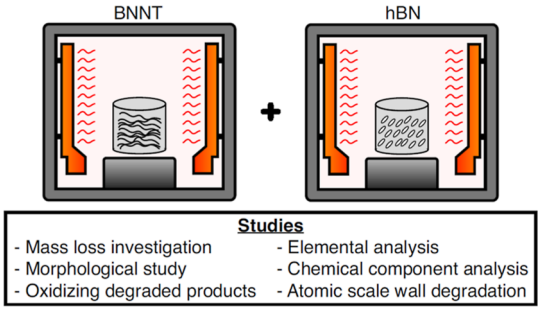

SEM imaging and energy-dispersive X-ray spectroscopy (EDS) were conducted using a Helios G4 UC (Thermo Fisher Scientific, Waltham, MA, USA) operating at 5 kV accelerating voltage with 100,000 magnification. EDS analysis was performed using the same instrument with an Oxford X-Max^N detector at 25,000 magnification to determine the elemental composition of samples before and after heat testing and oxidation. Iridium-coated samples were analyzed under SEM/EDS on an aluminum stub and a carbon tape. Therefore, these elements are removed from calculations. Three distinct sites were taken and analyzed for each sample to determine the average composition and are displayed in the Results section with their corresponding standard deviations as error bars. High-resolution transmission electron microscopy (HRTEM) imaging was carried out on a probe-aberration-corrected JEOL JEM-ARM200cF with a cold-field emission gun at 80 kV.

Oxidizing thermogravimetric analysis (OX-TGA) was carried out using a Q50 TGA (TA Instruments, New Castle, DE, USA) in air with a temperature ramp rate of 20 °C/min from 25 to 700 °C with a 20 min isothermal hold at 700 °C. About 10−15 mg mass of each sample was used for measurement. Fourier transform infrared spectroscopy (FTIR) was performed using a PerkinElmer Frontier FTIR/NIR with a conical sapphire attenuated total reflectance (ATR) accessory (Specac Golden Gate) at room temperature. A total of 8 accumulations were taken for each trial, and a background was taken to normalize the resultant spectra.

RESULTS AND DISCUSSION

Graphitic Furnace Heat Testing. In an inert environment, BNNTs and h-BN do not readily engage in many processes other than degradation. They would not oxidize quickly in the absence of oxygen, and neither boron nor nitrogen reacts with helium. The most likely undesired reaction is the formation of boron carbide from elemental

https://doi.org/10.1021/acsanm.2c01965
ACS Appl. Nano Mater. 2022, 5, 12444−12453

boron (from BNNT or h-BN) and carbon (from the graphite crucible). At high temperatures, the breakdown of boron nitride is believed to occur by the following process shown in eq 1.[20]

$$2\,BN_{(s)} \xrightarrow{\Delta} 2\,B_{(s)} + N_{2\,(g)} \quad (1)$$

At all temperatures relevant to this investigation, nitrogen is a gas that is easily taken away by the flowing helium in the graphitic furnace. Since pure boron has an extremely high boiling point of roughly 4000 °C, no substantial quantity of boron is believed to be evaporated during the heat-testing process.

The pictures of the heat-tested BNNT samples are shown in Figure 1. It can be easily seen that the pure white BNNTs change to a dark gray shade as the testing temperature rises. Throughout the range of increasing temperatures from 1800 to 2500 °C, the observed grayness of BNNTs is as follows: HT-BNNT 2500 > HT-BNNT 2200 > HT-BNNT 2000 > HT-BNNT 1800 > Neat BNNT. A similar trend of color change was observed in heat-tested h-BN samples but is not as pronounced as in BNNTs.

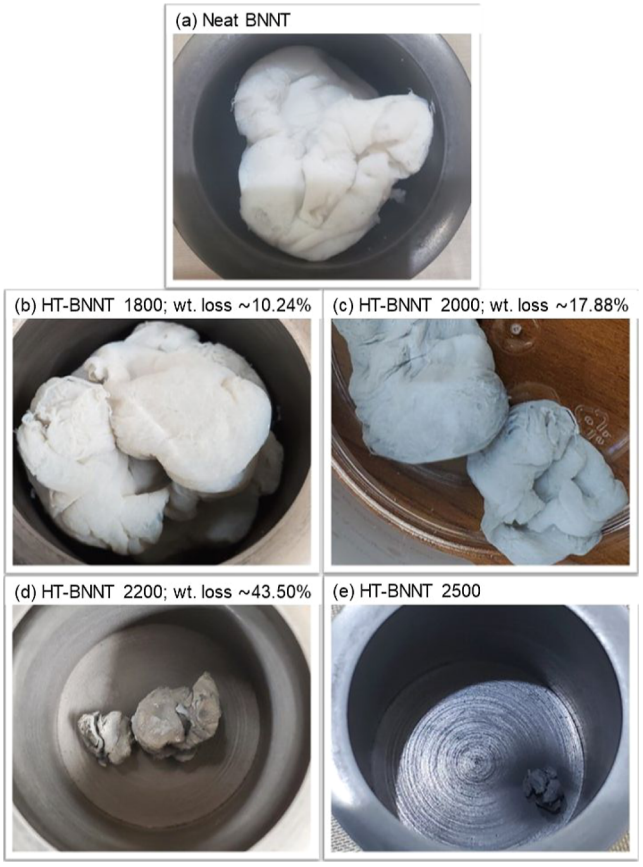

Figure 1. Pictures of (a) neat BNNTs and the heat-tested BNNT samples in the graphitic furnace at (b) 1800, (c) 2000, (d) 2200, and (e) 2500 °C. Pictures are of their natural color as captured. Weight loss shown in the picture is calculated from the measured weight of the sample before and after the test.

In addition to the observed color change, the weight loss measured after the furnace heat testing increases from ~10.24% for HT-BNNT 1800 to ~43.50% for HT-BNNT 2200. From Figure 1, it can be observed that the amount of the BNNT sample left after testing at 2500 °C is minimal. At 2500 °C, the left-over BNNT sample was a hard dark-gray mass. Although color changes in BNNTs can indicate the presence of boron, SEM imaging and EDS were conducted to produce a more detailed study of the morphology and identity of the remaining material.

High-Temperature Thermogravimetric Analysis. The high-temperature TGA (HT-TGA) results for BNNT samples heated to 2040 °C at 20 °C/min, paralleling the graphitic furnace heating procedure, are shown in Figure 2. Exhibiting complete stability of the BN nanotubular structure, BNNTs show negligible amounts of weight loss of 2.2% up to 1400 °C and 6.3% up to 1800 °C, the lowest temperature at which the samples were heat-tested. The rate of weight loss up to 1800 °C is less than 0.4%/°C. No significant peaks were found through derivative analysis. This small amount of weight loss, coupled with the negligible weight loss rate, is likely due to moisture content and defective sites in the BN structure that could cause early dissociation at 1800 °C. Furthermore, BNNTs show 12.5 and 17.8% weight loss at 2000 and 2040 °C, respectively. This significant weight loss can be attributed to the unzipping of outer walls as BN bonds may begin to dissociate. BNNT walls were observed and analyzed through TEM and other characterization methods to confirm dissociation.

The results and trends here align with the furnace heat-tested BNNT results. The weight loss values in the furnace-tested samples at 1800 and 2000 °C were ~10.24 and ~17.88%, compared to 6.3 and 12.5% for the HT-TGA, respectively. The slightly greater weight loss for the furnace-tested samples stems from the differences in weight measurement processes for each. The samples were weighed in the crucible before and after testing, so any small changes to the mass of the crucible itself, such as oxidation, will be shown in the weight loss measurements. The crucible for the furnace runs is also much heavier than for HT-TGA, ~50 g and ~150 mg, respectively; therefore, the small oxidation effect of the crucible due to impurity in purge gas would be more significant in the furnace runs. The HT-TGA measures weight loss throughout the run and employs a background subtraction measured from an identical run with the empty crucible. This will provide clearer results on the sample's mass loss as it is not confounded with the crucible effects. HT-TGA of h-BN (Figure 2) shows comparatively less weight loss than BNNTs with a slow and steady progressive loss with increasing temperature, explaining increased stability at high temperatures compared to BNNTs. The same trend in an oxidizing environment has been seen in the literature.[13,21] h-BN and BNNTs both show similar trends in weight loss throughout the temperature range. Up to 1400 °C, both BNNTs and h-BN show similar rates of weight loss with minimal overall weight loss, representing the stability of the BN bond in both layered and nanotubular structures. Between 1400 and 1800 °C, they start losing mass at the same time with BNNTs showing a higher rate of weight loss than h-BN. They both show a significant increase in weight loss rate after 1800 °C, with h-BN starting at ~1970 °C, slightly after BNNTs at ~1900 °C.

Scanning Electron Microscopy. Figure 3 shows SEM images of heat-tested BNNTs in the graphitic furnace compared with the neat, untested BNNTs. The BNNT entangled structure can be observed in the SEM, with h-BN appearing as circular, particle-like clusters. The h-BN is often found as non-tubular BN impurities in the purified BNNTs.

https://doi.org/10.1021/acsanm.2c01965
ACS Appl. Nano Mater. 2022, 5, 12444−12453

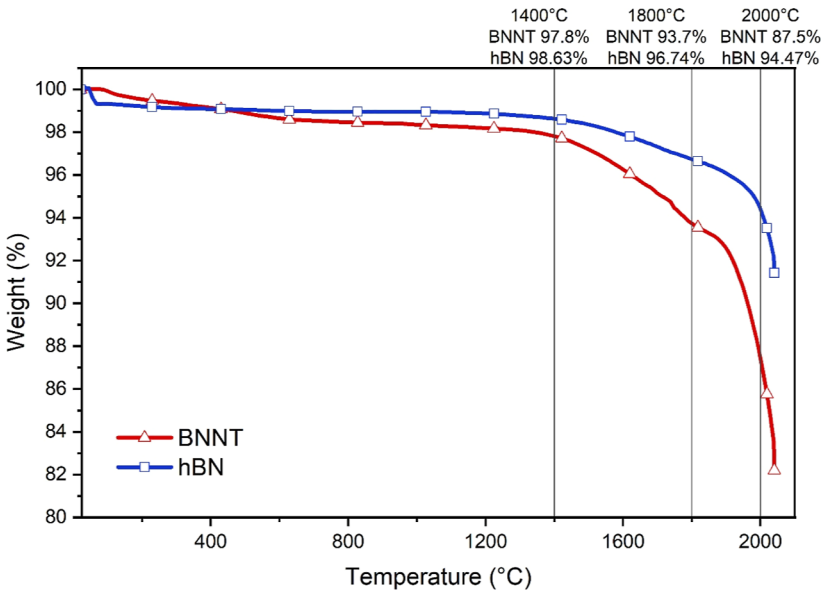

Figure 2. High-temperature TGA curve of purified BNNTs and h-BN.

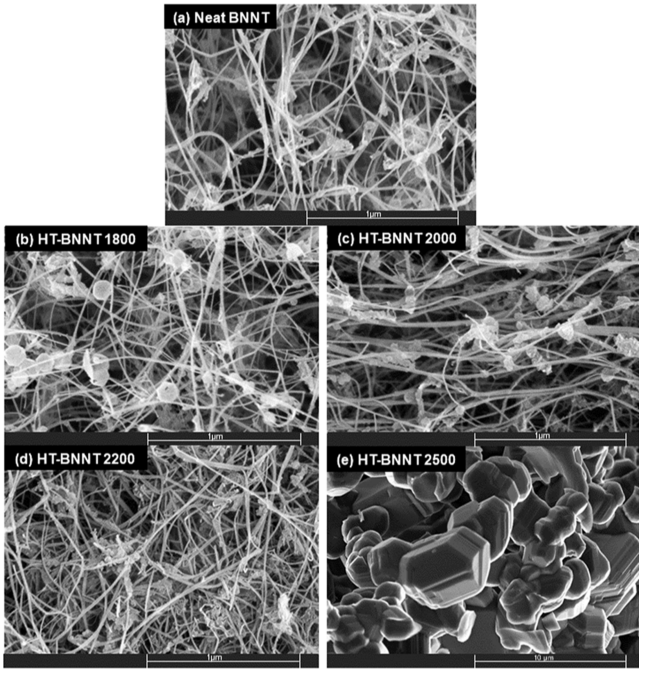

Figure 3. SEM images of (a) Neat BNNTs and heat-tested BNNTs at (b) 1800, (c) 2000, (d) 2200, and (e) 2500 °C.

The BNNT samples used in the experiment are the most purified and are expected to have about 50 wt % of h-BN as non-tubular impurities in purified neat BNNTs. SEM is a localized technique and does not describe the quantitative h-BN bulk content and may show visual differences in h-BN content in images. Despite the fact that BNNTs and h-BN have the same composition and bonding, they may show distinct thermal stability due to differing structures; hence, h-BN powder is separately examined for a comparative study to assess the effect of high temperature on BNNTs. Nanotube structures appear to have survived in the 1800, 2000, and 2200 °C furnace-tested samples with no distinguishable surface differences. The SEM shows that the heat-tested BNNTs at 2500 °C have dissociated and did not survive in tubular form (Figure 3e); nevertheless, at all other temperatures (Figure 3b–d), the structure of the nanotubes appears intact. However, the walls of multi-walled BNNTs may be damaged, which SEM imaging cannot detect. The HRTEM, OX-TGA, and EDS analyses were further performed to establish the entire survivability of walls up to 2200 °C.

Oxidizing Thermogravimetric Analysis. BNNTs and h-BN are completely stable up to 900 °C in an oxidative environment.[12] Before 700 °C, boron nitride does not dissociate or oxidize, but elemental boron and boron carbide oxidize to generate boron oxide.[22,23] Due to the dissociation of some layers of h-BN or BNNTs, elemental boron or boron-containing compounds, such as boron carbide, may be present in HT-BNNTs or HT-hBN samples. The projected weight gain due to the oxidation of elemental boron may be approximated using the following eqs 2 and 3.[24,25]

$$B_{(s)} + \frac{3}{4}O_{2\,(g)} \xrightarrow{\Delta} \frac{1}{1}B_2O_{3\,(s)} \tag{2}$$

$$1\ \text{g (B)} \cdot \frac{1\ \text{mole}}{10.81\ \text{g}} \cdot \frac{1\ \text{mole } B_2O_3}{2\ \text{mole B}} \cdot \frac{69.63\ \text{g}}{1\ \text{mole } B_2O_3} = 3.22\ \text{g } B_2O_3 \tag{3}$$

When oxidized, the sample gains 2.22 g of weight per 1 g of elemental boron. This weight gain is an upper limit estimate. Such a large percentage of relative weight gain also means that boron dissociated from boron nitride can make small amounts easier to detect. Boron oxide has traditionally been utilized as a protective layer to increase the oxidation resistance of carbon–carbon composites by restricting active sites and preventing oxygen transport.[26,27] Thus, newly forming boron oxide can create a layer surrounding the boron particle, protecting it from further oxidizing and not allowing elemental boron to gain weight fully.

A considerable weight increase of ~76% is seen in the OX-BNNT 2200 sample (Figure 4a). Unlike OX-BNNT 2200, all the other heat-tested or oxidized BNNT and h-BN samples behave similar to the OX-Neat BNNT sample and do not show any significant weight gain. The considerable weight gain

https://doi.org/10.1021/acsanm.2c01965
ACS Appl. Nano Mater. 2022, 5, 12444–12453

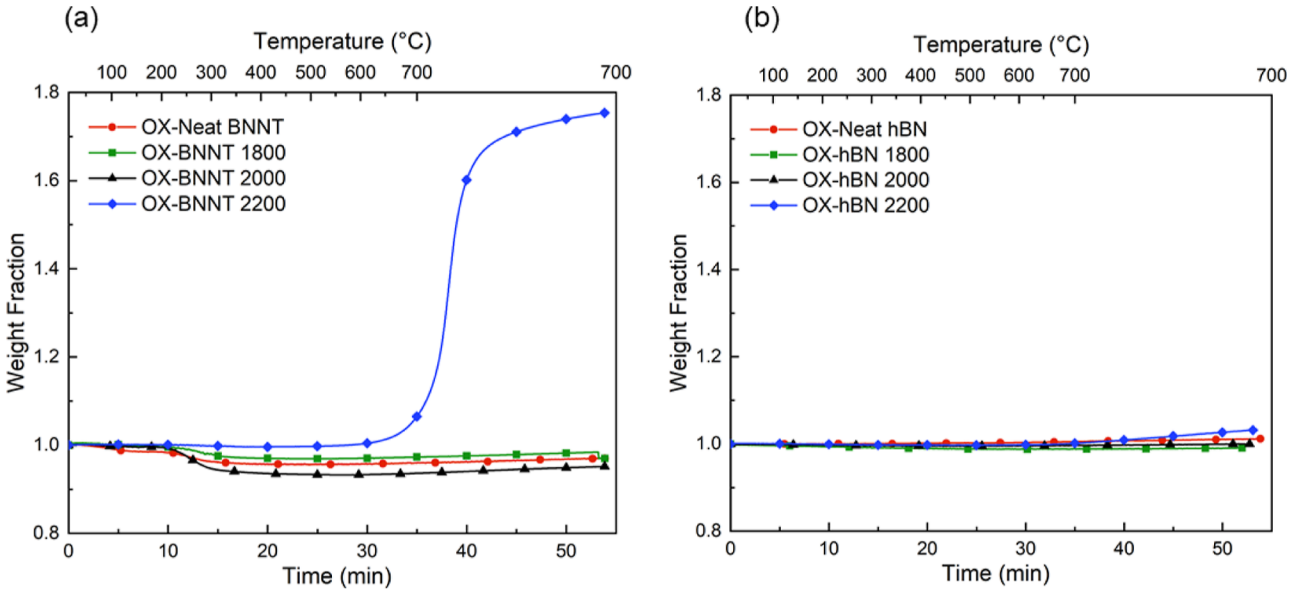

Figure 4. OX-TGA curves of oxidized (a) heat-tested BNNTs and (b) heat-tested h-BN.

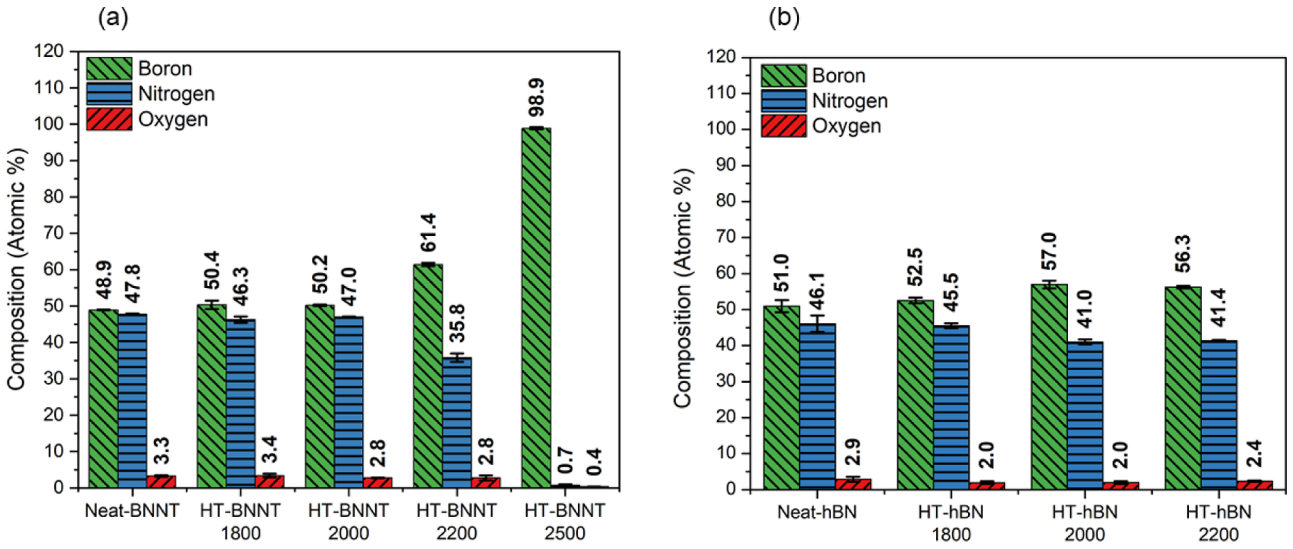

Figure 5. Atomic composition (%) for (a) heat-tested BNNT samples (HT-BNNT) and (b) heat-tested h-BN (HT-hBN).

shown only by the OX-BNNT 2200 sample indicates the presence of elemental boron upon heat testings exceeding 2000 °C. EDS analysis can be used to confirm the presence of elemental boron further.

Energy-Dispersive X-ray Spectroscopy. EDS is used to compare the existence of contributing elements in the BNNT heat-tested and oxidized materials. EDS measures chemical compositions directly and gives relative amounts of elements present in a sample.

Heat-Tested Samples. Results of the EDS analysis on heat-tested BNNTs and h-BN samples are summarized in Figure 5. As shown in Figure 5a, in samples: Neat BNNT, HT-BNNT 1800, and HT-BNNT 2000, the boron and nitrogen compositions hover steadily around 50 atomic %, with slight amounts of oxygen, up to 2000 °C. However, the boron atomic content suddenly increases by 11.2 atomic % from HT-BNNT 2000 to HT-BNNT 2200. The nitrogen content falls by the same amount as the increase of boron, but the oxygen content stays the same. As there is no alternative source of free boron, a proportionate and significant shift in atomic content suggests the dissociation of bonds within the tube walls.

The EDS data for HT-BNNT 2500 (Figure 5a) indicate 99% atomic content of elemental boron, indicating full breakdown of the B−N bond at 2500 °C. SEM imaging also captured this full decomposition, as shown in Figure 1d. Up to 2200 °C, the oxygen level of all neat and heat-tested samples remains identical, indicating that the heat testing did not cause oxidation.

The heat-tested h-BN samples, on the other hand, show a substantially more stable composition across the temperature range. The amount of boron content and weight loss in the sample increases slowly and steadily as the testing temperature rises. The h-BN possesses a surface area of ∼23 m^2/g,[21] while BNNTs have ∼180 m^2/g.[10] The many-layered structure of the h-BN sample and the lower surface area by a factor of ∼10 compared to the BNNT sample likely contribute to its greater stability. The number of bonds dissociated rises as the temperature rises, and the h-BN platelet loses layers. Layers

https://doi.org/10.1021/acsanm.2c01965
ACS Appl. Nano Mater. 2022, 5, 12444−12453

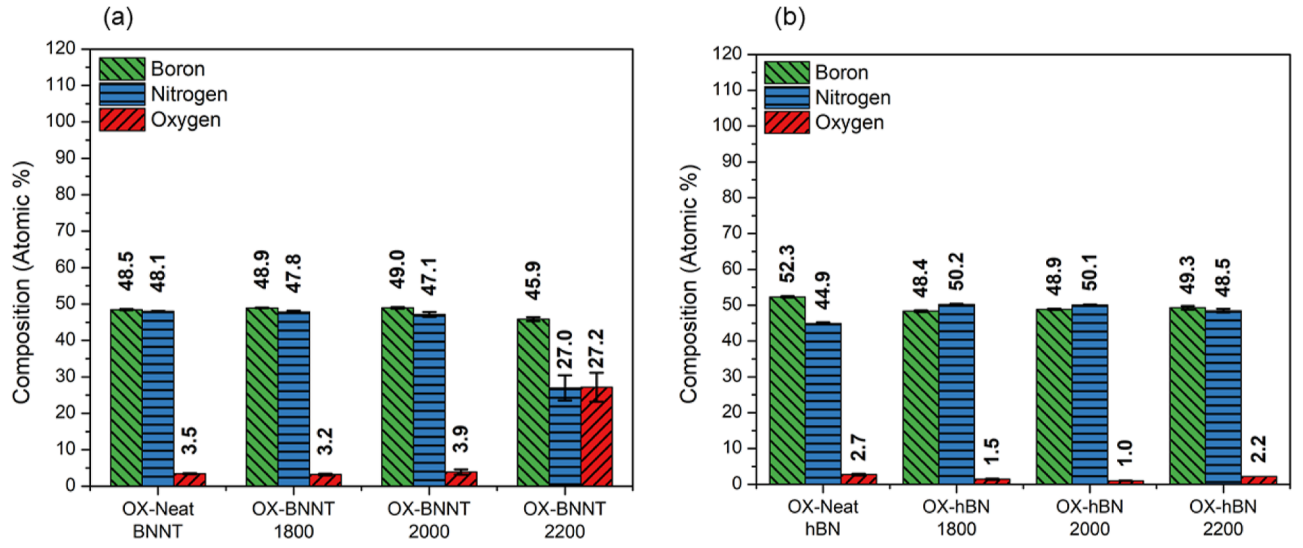

Figure 6. Atomic composition (%) for (a) oxidized BNNT samples and (b) oxidized h-BN samples.

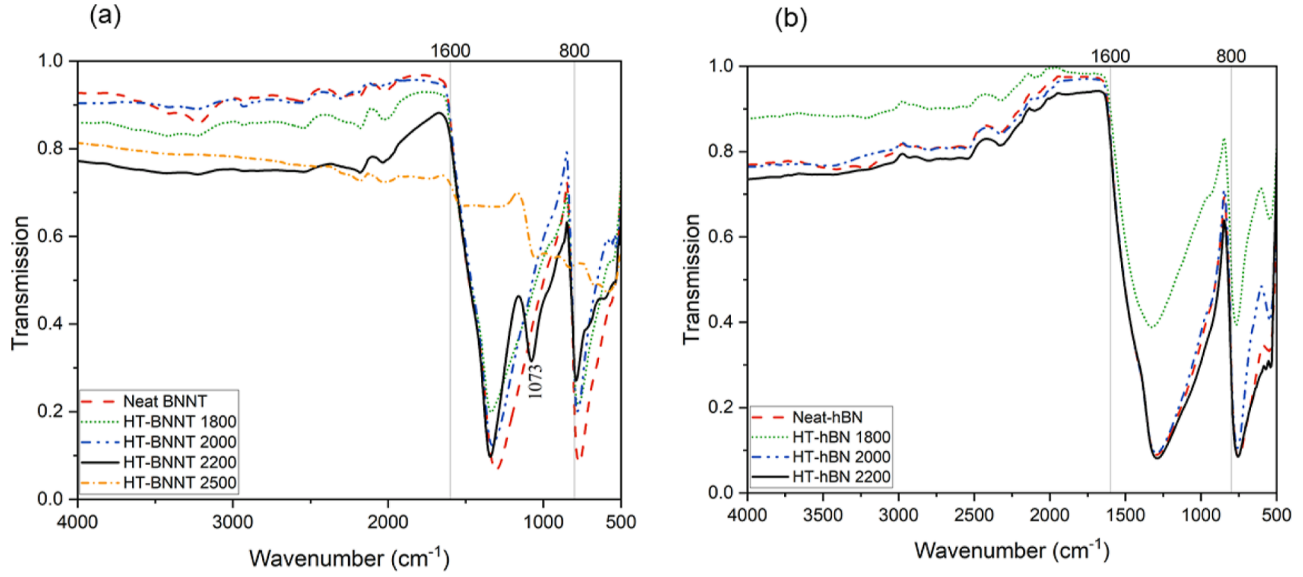

Figure 7. FTIR results for heat-tested (a) BNNT samples and (b) h-BN samples.

in h-BN platelets are held together through van der Waals interactions, whereas the layers themselves are chemically bonded.[28] This makes the layers more independent from one another and can aid in the thermal compositional stability of the bulk material. Even though methods for synthesizing monolayer and few-layered h-BN platelets have been established, they still typically have 2−10 layers.[28] However, in a few walled BNNT structures, the dissociation of a few BN links might cause an unzipping effect, leading to complete wall dissociation. Typically, h-BN has more layers than the number of walls in multi-walled BNNTs, which explains that the h-BN platelets can still exist after dissociating a few outer layers. Nevertheless, unzipping/dissociation of the same amount of walls in BNNTs may completely destroy a nanotube.

Heat-Tested and Oxidized Samples. A part of each heat-tested sample was oxidized via OX-TGA at 700 °C, and the resulting compositions observed through EDS analysis are summarized in Figure 6.

Up to 2000 °C, the OX-BNNT and OX-hBN samples exhibit no substantial increase in oxygen content after oxidation, indicating the absence of elemental boron in the samples heat-tested to temperatures up to 2000 °C. The oxygen content of the BNNT 2200 sample significantly increases from 2.8% (HT-BNNT 2200, Figure 5a) to 27.2% (OX-BNNT 2200, Figure 6a). The atomic fraction of boron exceeds nitrogen by 18.9% in the OX-BNNT 2200 sample. This excess of 18.9% boron and the 27.2% oxygen represents the stoichiometry of B_2O_3. Furthermore, this explains the survival of BN compounds at temperatures as high as 2200 °C. We presume that the majority of the oxygen content in the BNNT and h-BN samples after oxidation resulted from the oxidation of elemental boron or boron carbide since BNNTs and h-BN are unlikely to oxidize much before 700 °C. This considerable increase in oxygen content through oxidation of HT-BNNT 2200 indicates the presence of elemental boron in the HT-BNNT 2200 sample through dissociation of the B−N bond after exposure to heat testing at 2200 °C. The OX-hBN samples do not show a substantial gain in oxygen content (Figure 6b), providing further evidence of the destruction or unzipping of some layers of BNNTs but not of h-BN at 2200

https://doi.org/10.1021/acsanm.2c01965
ACS Appl. Nano Mater. 2022, 5, 12444−12453

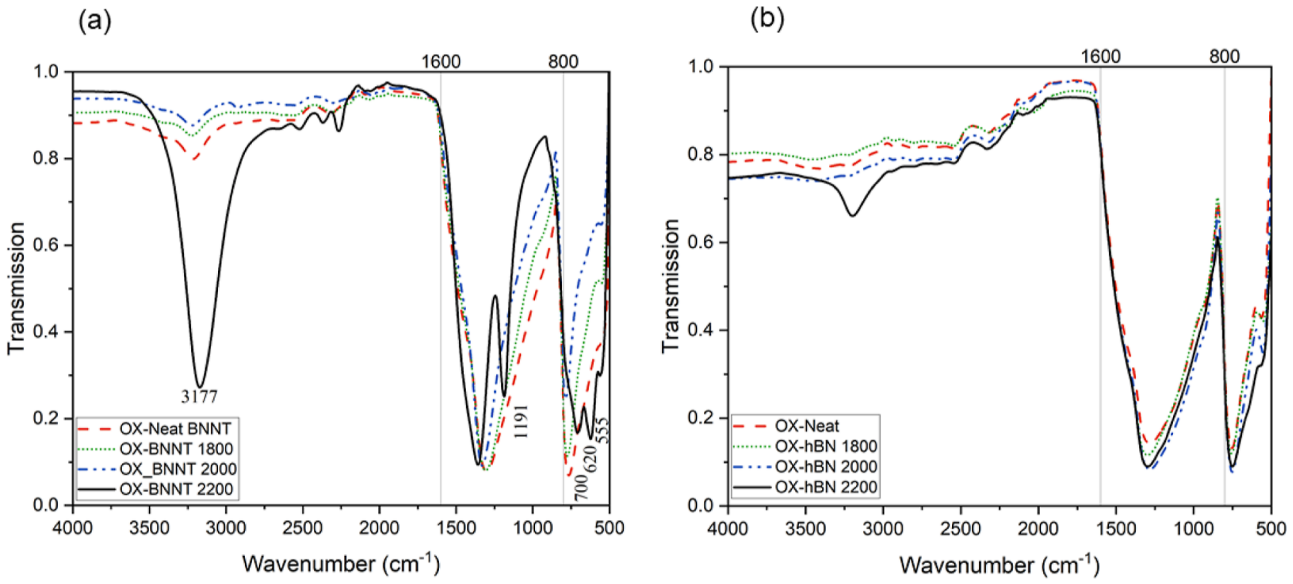

Figure 8. FTIR results for (a) oxidized heat-tested BNNT samples and (b) oxidized heat-tested h-BN samples.

°C. The presence of elemental boron at 2200 °C in BNNT but not in h-BN, even though they possess the same chemistry, explains that the individual BN layers unzipped from BNNTs due to temperature effects can be readily dissociated into elemental boron and nitrogen at high temperatures compared to the stacked BN layers as in h-BN.

Fourier Transform Infrared Spectroscopy. FTIR spectroscopy is used to determine compounds and bonds that are present in a sample. The peak location (wavenumber) is a function of bond vibrations and can be used to determine the chemical bonds. This is useful in building on results found by EDS and confirming whether other reactions are occurring during heat testing and oxidation.

Heat-Tested Samples. Figure 7 shows the FTIR curves for heat-tested BNNTs and h-BN. Two characteristic broadband B−N bond peaks can be seen in Figure 7a,b: first for out-of-plane buckling perpendicular to the tube axis at low wavenumbers between 500 and 800 cm^{-1} and another for in-plane optical phonon modes parallel to the tube axis at high wavenumbers between 800 and 1600 cm^{-1}.[29−34] Figure 7a shows the characteristic peaks for HT-BNNTs, and Figure 7b shows HT-hBN samples. For heat-tested BNNTs at 2500 °C, FTIR shows the absence of B−N bond characteristic peaks. As depicted from the SEM imaging (Figure 3d) and EDS results (Figure 5a), FTIR further confirms the complete dissociation of B−N bonds at 2500 °C through the absence of B−N characteristic peaks. B−N bond characteristic peaks are present for all other levels of testing temperature (1800, 2000, and 2200 °C), indicating the survival of BNNTs and h-BN until 2200 °C temperature for the most part.

Carbon tape was used in the sample preparation for SEM/EDS analysis. Any elemental carbon captured through the EDS analysis will be from the combination of (1) carbon compounds formed during heating by the reaction of carbon from the crucible and boron or boron nitride from the sample, (2) unreacted residual elemental carbon particles on the sample from the carbon crucible, and (3) carbon from the carbon tape used for the sample preparation. Carbon atomic analysis through EDS cannot distinguish between these reasons for carbon existence. Some samples or sites with less thickness will show more carbon content in EDS analysis as it will capture from the bottom carbon tape. Such samples or sites may also show the aluminum content from the aluminum stub used for sample preparation. Therefore, elemental carbon, aluminum, and iridium (coating material) were removed from the EDS calculations and not depicted in the EDS map results. However, this limitation of not capturing carbon presence due to formation of carbon compounds through EDS is covered by FTIR analysis. The HT-BNNT 2200 sample shows a characteristic icosahedral boron carbide vibration peak at 1073 cm^{-1}.[35] The existence of a visible boron carbide peak for the HT-BNNT 2200 sample indicates that at around 2200 °C, dissociated elemental boron interacted with carbon from the graphite crucible to generate a potentially small amount of boron carbide. Furthermore, no other samples showed the carbide peak, proving BN does not react with the crucible carbon. However, elemental boron formed through dissociation reacted with carbon from the crucible as captured through FTIR. These FTIR observations align with the results from OX-TGA and EDS analyses.

Heat-Tested and Oxidized Samples. Figure 8 shows the FTIR curves for the heat-tested and oxidized samples of BNNT and h-BN. Up to 2000 °C, the FTIR curves for OX-BNNT (Figure 8a) and OX-hBN (Figure 8b) samples indicate no major peaks other than two B−N bond peaks between 500−800 and 800−1600 cm^{-1}. However, the oxidized BNNT, OX-BNNT 2200 (Figure 8a), shows strong peaks corresponding to boron oxide compounds at 3177, 1191, 620−, and 555 cm^{-1}.[29,35,36] Completely agreeing with the OX-TGA (Figure 4a) and EDS results (Figure 6a), FTIR indicates the presence of elemental boron or boron carbide in BNNT at 2200 °C by showing oxidized boron compounds in OX-BNNT 2200. The absence of boron oxide in OX-BNNTs up to 2000 °C confirms the stability of B−N bonds in BNNTs up to 2000 °C. In contrast to the OX-BNNT 2200 sample, OX-hBN 2200 shows only a slight peak at 3191 cm^{-1} with the absence of other oxidized compound peaks, representing the stability of h-BN up to 2200 °C with dissociation of few layers.

High-Resolution Transmission Electron Microscopy. HRTEM images of BNNTs can be seen in Figure 9. The

https://doi.org/10.1021/acsanm.2c01965
ACS Appl. Nano Mater. 2022, 5, 12444−12453

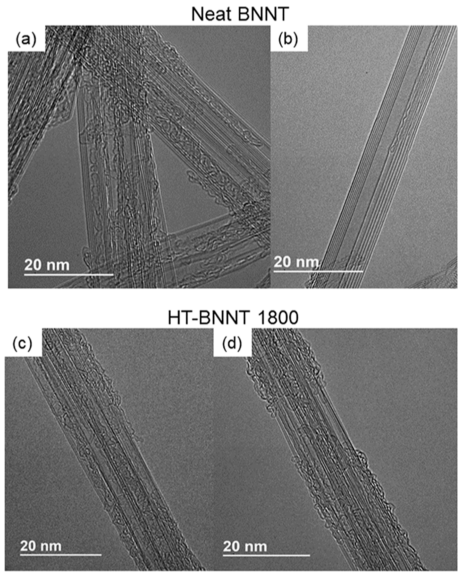

Figure 9. HRTEM images of (a,b) neat/untested BNNTs and (c,d) heat-tested BNNTs at 1800 °C. All the images are at the same magnification, with the scale bar shown at the bottom of the image.

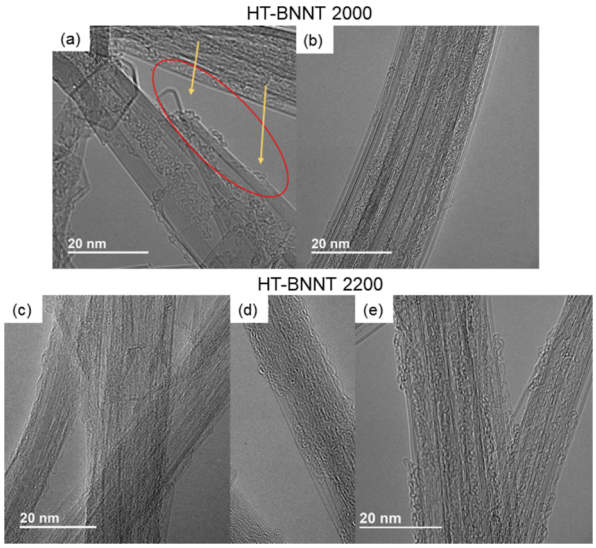

Figure 10. HRTEM images of (a,b) heat-tested BNNT at 2000 °C showing few walls damaged in a red circle marked by yellow arrows and (c−e) heat-tested BNNT at 2200 °C. All the images are at the same magnification, with the scale bar shown at the bottom of the image.

typical multi-walled tube nature is shown, often exhibiting five or more walls, with an amorphous structure seen at the tubes' surface and potentially inside the hollow tubes. The clusters observed through TEM around the tubes (as seen in Figure 9a) are most likely amorphous BN species clusters.[37,38] HRTEM images of the HT-BNNT 1800 sample (Figure 9c,d) show preserved high crystalline structure of BNNTs after the exposure up to 1800 °C. No wall damage or nanotube cutting was found in TEM for the HT-BNNT 1800 sample explaining the complete stability of BNNTs up to 1800 °C temperature exposure.

The previously observed weight loss of 12.5% at 2000 °C through HT-TGA suggested few unzipping or dissociation of the walls. This assumption can be confirmed through HRTEM image analysis showing specific wall damage at 2000 °C, as shown in Figure 10a. For 2000 °C (HT-BNNT 2000), a negligible increment in the atomic level of elemental boron was seen through EDS, as discussed before, explaining that very few walls dissociated at 2000 °C. From various TEM images at different magnifications, ∼30−35 tubes were closely examined, out of which 2−3 nanotubes were observed to have outer wall damage, explaining that the outer walls of about <10% of nanotubes were affected due to heat testing at 2000 °C. During the synthesis process, there is a chance of having damaged wall tubes in the as-produced BNNTs. However, the TEM analysis on neat samples did not capture any suspicion of such damaged tubes. In addition, such tubes with pre-existing damaged walls or defects are more likely to dissociate earlier when exposed to heat. Suspected existence of survived damaged tube walls in the heat-treated sample at 2000 °C during TEM analysis suggests that the tubes are more likely damaged during the heat treatment. By showing the survival of highly crystalline tubular structure (Figure 10b) and minimal wall damage (Figure 10a) for HT-BNNT 2000, TEM image analysis entirely agrees with the previously observed results through HT-TGA, OX-TGA, EDS, and FTIR. At 2200 °C, many amorphous boron clusters are seen through TEM (Figure 10c,d). These additional amorphous boron clusters, also captured through all previous analyses, suggest the dissociation of BNNTs in abundant amounts. Color darkening, a weight loss of ∼43.5% and an increased boron atomic level upon furnace heating, significant weight gain upon oxidation, presence of boron oxide compounds in an oxidized sample, and observation of boron clusters at the nanoscale together reveal that BNNTs did not entirely survive 2200 °C temperature exposure.

SUMMARY AND CONCLUSIONS

Here, we presented the first study investigating the extreme temperature thermal behavior and degradation mechanisms of BNNTs in an inert environment. Through heat testing and subsequent characterization, it was found that BNNTs remain wholly stable at temperatures up to 1800 °C. HRTEM confirmed excellent wall retention and crystallinity with insignificant weight loss observed through HT-TGA; also, no evidence of elemental boron was found during oxidation characterization. After heat testing at 2000 °C, EDS and FTIR analyses did not show any indications of the presence of elemental boron; however, the sample lost 12.5% weight during HT-TGA at 2000 °C. This indicates the possibility of partial wall damage and unzipping of walls, which was confirmed through HRTEM imaging.

At 2200 °C, a large fraction of BNNTs survived, but a significant fraction was also lost to dissociation of the BN bond, indicated by a weight loss of ∼43.5%. The increase in boron captured through EDS matched the loss in nitrogen and is compelling evidence for the dissociation of the stoichiometrically equal BN bond. Furthermore, significant boron oxide peaks in oxidized samples found through FTIR analysis confirmed the formation of elemental boron during heat testing at 2200 °C. At 2500 °C, BNNTs did not survive in tubular form and completely dissociated into amorphous boron and nitrogen gas.

The heat-tested h-BN samples, on the other hand, showed a far more consistent composition throughout a wider temperature range. As the testing temperature rises, the level of boron content and weight loss in the sample increases slowly and

https://doi.org/10.1021/acsanm.2c01965
ACS Appl. Nano Mater. 2022, 5, 12444−12453

gradually. The h-BN's many-layered nature likely contributes to its stability. The h-BN platelets can still survive after dissociating a few outer layers as h-BN typically has more layers than the number of walls in multi-walled BNNTs. In comparison, the failure of just a few BN bonds in a few-walled BNNT may induce unzipping, exposing monolayers of BN to the heat, rapidly accelerating the degradation of the tube. An interesting area for further study will be to investigate whether certain regions of an individual HTP BNNT are more resistant to heat than others. In the HTP method, an individual tube forms under time-varying thermodynamic conditions. It is likely that the one end of a BNNT may have fewer defects than the other and hence be more stable, suggesting that inert gas testing might be used as a method of purification by weeding out the more defective sections of the tubes first.

The evidence of BNNT stability in inert environments should encourage the incorporation of BNNTs into new matrices with harsh processing conditions. The sintering process of ceramics is extremely harsh and has limited the use of filler materials. With high thermal conductivity, excellent mechanical properties, and thermal stability at extreme temperatures, BNNTs could be of great benefit for ceramic matrix composites along with polymer and metal matrix composites. This novel, fundamental study of decomposition at extreme temperature is a basis for BNNT nanocomposite research and future harsh environment applications.

■ ASSOCIATED CONTENT

Supporting Information

The Supporting Information is available free of charge at https://pubs.acs.org/doi/10.1021/acsanm.2c01965.

Additional details of boron nitride nanopowder (h-BN) as-received material and SEM images (PDF)

■ AUTHOR INFORMATION

Corresponding Author

Rebekah D. Sweat − *FAMU-FSU College of Engineering, Tallahassee, Florida 32310, United States; High-Performance Materials Institute (HPMI), Tallahassee, Florida 32310, United States*; Email: r.sweat@eng.famu.fsu.edu

Authors

Mehul J. Tank − *FAMU-FSU College of Engineering, Tallahassee, Florida 32310, United States; High-Performance Materials Institute (HPMI), Tallahassee, Florida 32310, United States*; orcid.org/0000-0002-6011-0354

Aspen N. Reyes − *FAMU-FSU College of Engineering, Tallahassee, Florida 32310, United States; High-Performance Materials Institute (HPMI), Tallahassee, Florida 32310, United States*

Jin Gyu Park − *FAMU-FSU College of Engineering, Tallahassee, Florida 32310, United States; High-Performance Materials Institute (HPMI), Tallahassee, Florida 32310, United States*

Lyndsey R. Scammell − *BNNT Materials, Newport News, Virginia 23606, United States*; orcid.org/0000-0002-7133-7546

Michael W. Smith − *BNNT Materials, Newport News, Virginia 23606, United States*

Ana De Leon − *FAMU-FSU College of Engineering, Tallahassee, Florida 32310, United States; High-Performance Materials Institute (HPMI), Tallahassee, Florida 32310, United States*; orcid.org/0000-0003-0847-7412

Complete contact information is available at: https://pubs.acs.org/10.1021/acsanm.2c01965

Author Contributions

The manuscript was written through contributions of all authors. All authors have given approval to the final version of the manuscript.

Funding

This research was funded by Florida State University start-up funds.

Notes

The authors declare no competing financial interest.

■ ACKNOWLEDGMENTS

The authors would like to thank the National High-Magnetic Field Laboratory for TEM and SEM support. TEM work was performed by Dr. Yan Xin at the National High Magnetic Field Laboratory, which is supported by the National Science Foundation Cooperative Agreement no. DMR-1644779, and the State of Florida. The authors would also like to thank Dr. Daniel Hallinan and Micah Silverman for the use and support of FTIR measurements, Matthew Wadsworth for the support and guidance for EDS analysis, and Matthew Lundblad for the assistance with the high-temperature furnace.

■ ABBREVIATIONS

neat BNNT/hBN, untested or as-received BNNT or h-BN

HT-BNNT/hBN 1800, heat-tested BNNT or h-BN in graphitic furnace up to 1800 °C

OX-neat BNNT/hBN, Post oxidizing TGA of untested or as-received BNNT or h-BN in air

OX-BNNT/hBN 1800, post oxidizing TGA of BNNT or h-BN in air

■ REFERENCES

(1) Blase, X.; Rubio, A.; Louie, S. G.; Cohen, M. L. Stability and Band Gap Constancy of Boron Nitride Nanotubes. *Europhys. Lett.* **1994**, *28*, 335−340.

(2) Rubio, A.; Corkill, J. L.; Cohen, M. L. Theory of Graphitic Boron Nitride Nanotubes. *Phys. Rev. B: Condens. Matter Mater. Phys.* **1994**, *49*, 5081−5084.

(3) Chopra, N. G.; Luyken, R. J.; Cherrey, K.; Crespi, V. H.; Cohen, M. L.; Louie, S. G.; Zettl, A. Boron Nitride Nanotubes. *Science* **1995**, *269*, 966.

(4) Wei, X.; Wang, M.-S.; Bando, Y.; Golberg, D. Tensile Tests on Individual Multi-Walled Boron Nitride Nanotubes. *Adv. Mater.* **2010**, *22*, 4895−4899.

(5) Chopra, N. G.; Zettl, A. Measurement of the elastic modulus of a multi-wall boron nitride nanotube. *Solid State Commun.* **1998**, *105*, 297.

(6) Arenal, R.; Wang, M.-S.; Xu, Z.; Loiseau, A.; Golberg, D. Young Modulus, Mechanical and Electrical Properties of Isolated Individual and Bundled Single-Walled Boron Nitride Nanotubes. *Nanotechnology* **2011**, *22*, 265704.

(7) Tanur, A. E.; Wang, J.; Reddy, A. L. M.; Lamont, D. N.; Yap, Y. K.; Walker, G. C. Diameter-Dependent Bending Modulus of Individual Multiwall Boron Nitride Nanotubes. *J. Phys. Chem. B* **2013**, *117*, 4618−4625.

(8) Turhan, E. A.; Pazarçeviren, A. E.; Evis, Z.; Tezcaner, A. Properties and Applications of Boron Nitride Nanotubes. *Nanotechnology* **2022**, *33*, 242001.
(9) Xu, T.; Zhang, K.; Cai, Q.; Wang, N.; Wu, L.; He, Q.; Wang, H.; Zhang, Y.; Xie, Y.; Yao, Y.; Chen, Y. Advances in Synthesis and Applications of Boron Nitride Nanotubes: A Review. *Chem. Eng. J.* **2022**, *431*, 134118.
(10) Kostoglou, N.; Tampaxis, C.; Charalambopoulou, G.; Constantinides, G.; Ryzhkov, V.; Doumanidis, C.; Matovic, B.; Mitterer, C.; Rebholz, C. Boron Nitride Nanotubes Versus Carbon Nanotubes: A Thermal Stability and Oxidation Behavior Study. *Nanomaterials* **2020**, *10*, 2435.
(11) Zhi, C.; Bando, Y.; Tang, C.; Golberg, D. Boron Nitride Nanotubes. *Mater. Sci. Eng. R Rep.* **2010**, *70*, 92−111.
(12) Chen, Y.; Zou, J.; Campbell, S. J.; Le Caer, G. Boron Nitride Nanotubes: Pronounced Resistance to Oxidation. *Appl. Phys. Lett.* **2004**, *84*, 2430−2432.
(13) Chen, X.; Dmuchowski, C. M.; Park, C.; Fay, C. C.; Ke, C. Quantitative Characterization of Structural and Mechanical Properties of Boron Nitride Nanotubes in High Temperature Environments. *Sci. Rep.* **2017**, *7*, 11388.
(14) Ghassemi, H. M.; Lee, C. H.; Yap, Y. K.; Yassar, R. S. In Situ TEM Monitoring of Thermal Decomposition in Individual Boron Nitride Nanotubes. *J. Occup. Med.* **2010**, *62*, 69.
(15) Xu, Z.; Golberg, D.; Bando, Y. In Situ TEM-STM Recorded Kinetics of Boron Nitride Nanotube Failure under Current Flow. *Nano Lett.* **2009**, *9*, 2251−2254.
(16) Tiano, A. L.; Park, C.; Lee, J. W.; Luong, H. H.; Gibbons, L. J.; Chu, S.-H.; Applin, S.; Gnoffo, P.; Lowther, S.; Kim, H. J.; Danehy, P. M.; Inman, J. A.; Jones, S. B.; Kang, J. H.; Sauti, G.; Thibeault, S. A.; Yamakov, V.; Wise, K. E.; Su, J.; Fay, C. C. *Boron Nitride Nanotube: Synthesis and Applications*; Varadan, V. K., Ed.: San Diego, California, USA, 2014; p 906006.
(17) Cho, H.; Walker, S.; Plunkett, M.; Ruth, D.; Iannitto, R.; Martinez Rubi, Y.; Kim, K. S.; Homenick, C. M.; Brinkmann, A.; Couillard, M.; Dénommée, S.; Guan, J.; Jakubinek, M. B.; Jakubek, Z. J.; Kingston, C. T.; Simard, B. Scalable Gas-Phase Purification of Boron Nitride Nanotubes by Selective Chlorine Etching. *Chem. Mater.* **2020**, *32*, 3911−3921.
(18) Paige, C.; Newman, D.; Lombardo, S. J. H. An Integrated Innovative 3D Radiation Protection Fabric for Advanced Spacesuits and Systems. *IEEE Aerospace Conference*; IEEE: Big Sky: MT, USA, 2020; pp 1−11.
(19) Thibeault, S. A.; Kang, J. H.; Sauti, G.; Park, C.; Fay, C. C.; King, G. C. Nanomaterials for Radiation Shielding. *MRS Bull.* **2015**, *40*, 836−841.
(20) Dreger, L. H.; Dadape, V. V.; Margrave, J. L. Sublimation and decomposition studies on boron nitride and aluminum nitride1. *J. Phys. Chem.* **1962**, *66*, 1556−1559.
(21) Kostoglou, N.; Polychronopoulou, K.; Rebholz, C. Thermal and Chemical Stability of Hexagonal Boron Nitride (h-BN) Nanoplatelets. *Vacuum* **2015**, *112*, 42−45.
(22) Amin, M. S.; Molin, T. E.; Tampubolon, C.; Kranbuehl, D. E.; Schniepp, H. C. Boron Nitride Nanotube Impurity Detection and Purity Verification. *Chem. Mater.* **2020**, *32*, 9090−9097.
(23) Litz, L. M.; Mercuri, R. A. Oxidation of Boron Carbide by Air, Water, and Air-Water Mixtures at Elevated Temperatures. *J. Electrochem. Soc.* **1963**, *110*, 921.
(24) Rizzo, H. F. Oxidation of Boron at Temperatures between 400 and 1300°C in Air. *Boron Synthesis, Structure, and Properties*; Springer US: Boston, MA, 1960; pp 175−189.
(25) Jain, A.; Joseph, K.; Anthonysamy, S.; Gupta, G. S. Kinetics of Oxidation of Boron Powder. *Thermochim. Acta* **2011**, *514*, 67−73.
(26) Sogabe, T.; Okada, O.; Kuroda, K.; Inagaki, M. Improvement in Properties and Air Oxidation Resistance of Carbon Materials by Boron Oxide Impregnation. *Carbon* **1997**, *35*, 67−72.
(27) Savchenko, D. V.; Serdan, A. A.; Morozov, V. A.; Van Tendeloo, G.; Ionov, S. G. Improvement of the Oxidation Stability and the Mechanical Properties of Flexible Graphite Foil by Boron Oxide Impregnation. *N. Carbon Mater.* **2012**, *27*, 12−18.
(28) Pacilé, D.; Meyer, J. C.; Girit, Ç. Ö.; Zettl, A. The Two-Dimensional Phase of Boron Nitride: Few-Atomic-Layer Sheets and Suspended Membranes. *Appl. Phys. Lett.* **2008**, *92*, 133107.
(29) Liao, Y.; Chen, Z.; Connell, J. W.; Fay, C. C.; Park, C.; Kim, J.-W.; Lin, Y. Chemical Sharpening, Shortening, and Unzipping of Boron Nitride Nanotubes. *Adv. Funct. Mater.* **2014**, *24*, 4497−4506.
(30) Kim, D.; Nakajima, S.; Sawada, T.; Iwasaki, M.; Kawauchi, S.; Zhi, C.; Bando, Y.; Golberg, D.; Serizawa, T. Sonication-Assisted Alcoholysis of Boron Nitride Nanotubes for Their Sidewalls Chemical Peeling. *Chem. Commun.* **2015**, *51*, 7104−7107.
(31) Lee, C. H.; Wang, J.; Kayatsha, V. K.; Huang, J. Y.; Yap, Y. K. Effective Growth of Boron Nitride Nanotubes by Thermal Chemical Vapor Deposition. *Nanotechnology* **2008**, *19*, 455605.
(32) Shin, H.; Guan, J.; Zgierski, M. Z.; Kim, K. S.; Kingston, C. T.; Simard, B. Covalent Functionalization of Boron Nitride Nanotubes via Reduction Chemistry. *ACS Nano* **2015**, *9*, 12573−12582.
(33) Rozenberg, A. S.; Sinenko, Yu. A.; Chukanov, N. V. IR Spectroscopy Characterization of Various Types of Structural Irregularities in Pyrolytic Boron Nitride. *J. Mater. Sci.* **1993**, *28*, 5675−5678.
(34) Tang, C.; Bando, Y.; Zhi, C.; Golberg, D. Boron−Oxygen Luminescence Centres in Boron−Nitrogen Systems. *Chem. Commun.* **2007**, *44*, 4599.
(35) Li, X.; Jiang, D.; Zhang, J.; Lin, Q.; Chen, Z.; Huang, Z. The Dispersion of Boron Carbide Powder in Aqueous Media. *J. Eur. Ceram. Soc.* **2013**, *33*, 1655−1663.
(36) Nautiyal, P.; Loganathan, A.; Agrawal, R.; Boesl, B.; Wang, C.; Agarwal, A. Oxidative Unzipping and Transformation of High Aspect Ratio Boron Nitride Nanotubes into "White Graphene Oxide" Platelets. *Sci. Rep.* **2016**, *6*, 29498.
(37) Shimizu, Y.; Moriyoshi, Y.; Tanaka, H.; Komatsu, S. Boron Nitride Nanotubes, Webs, and Coexisting Amorphous Phase Formed by the Plasma Jet Method. *Appl. Phys. Lett.* **1999**, *75*, 929−931.
(38) Huang, J. Y.; Zhu, Y. T. Atomic-Scale Structural Investigations on the Nucleation of Cubic Boron Nitride from Amorphous Boron Nitride under High Pressures and Temperatures. *Chem. Mater.* **2002**, *14*, 1873−1878.

https://doi.org/10.1021/acsanm.2c01965
ACS Appl. Nano Mater. 2022, 5, 12444−12453